Petroleum Science 22 (2025) 3293–3303

Contents lists available at ScienceDirect

Petroleum Science

journal homepage: www.keaipublishing.com/en/journals/petroleum-science

Original Paper

# The analysis of drill string dynamics for extra-deep wells based on successive over-relaxation node iteration method

Wen-Chang Wang [a,b,c], He-Yuan Yang [c], Da-Kun Luo [c], Ming-Ming You [c], Xing Zhou [c], Feng Chen [d,*], Qin-Feng Di [b,c,**]

[a] *Shanghai Key Laboratory of Mechanics in Energy Engineering, Shanghai, 200072, China*
[b] *Shanghai Institute of Applied Mathematics and Mechanics, Shanghai, 200072, China*
[c] *School of Mechanics and Engineering Science, Shanghai University, Shanghai, 200072, China*
[d] *School of Mechatronics Engineering and Automation, Shanghai University, Shanghai, 200444, China*

ARTICLE INFO

*Article history:*
Received 6 January 2025
Received in revised form
27 May 2025
Accepted 28 May 2025
Available online 30 May 2025

Edited by Jia-Jia Fei

*Keywords:*
Extra-deep well
Drill string dynamics
Calculation speed-up method
SOR iteration method

ABSTRACT

The complex vibration directly affects the dynamic safety of drill string in ultra-deep wells and extra-deep wells. It is important to understand the dynamic characteristics of drill string to ensure the safety of drill string. Due to the super slenderness ratio of drill string, strong nonlinearity implied in dynamic analysis and the complex load environment, dynamic simulation of drill string faces great challenges. At present, many simulation methods have been developed to analyze drill string dynamics, and node iteration method is one of them. The node iteration method has a unique advantage in dealing with the contact characteristics between drill string and borehole wall, but its drawback is that the calculation consumes a considerable amount of time. This paper presents a dynamic simulation method of drilling string in extra-deep well based on successive over-relaxation node iterative method (SOR node iteration method). Through theoretical analysis and numerical examples, the correctness and validity of this method were verified, and the dynamics characteristics of drill string in extra-deep wells were calculated and analyzed. The results demonstrate that, in contrast to the conventional node iteration method, the SOR node iteration method can increase the computational efficiency by 48.2% while achieving comparable results. And the whirl trajectory of the extra-deep well drill string is extremely complicated, the maximum rotational speed downhole is approximately twice the rotational speed on the ground. The dynamic torque increases rapidly at the position of the bottom stabilizer, and the lateral vibration in the middle and lower parts of drill string is relatively intense.


## 1. Introduction

The geological conditions encountered in the ultra-deep (with a vertical depth exceeding 6000 m) oil and gas resource drilling are complex, and there are high drilling safety risks, long periods and numerous difficulties. One of the most typical problems is how to ensure the drill string safety. To solve this conundrum, aside from enhancing the quality and strength of drilling implements, numerous scholars have initiated calculations and measurements of the dynamic characteristics of drill strings in ultra-deep wells (with well depths ranging from 6000 to 9000 m), and have been exerting efforts to undertake research on drill string vibration control methods. The subjects of these studies involved uniaxial vibration, bi-axial coupling and tri-axial coupling vibration of drill string (Moraes and Savi, 2018; Naganawa, 2012; Ritto et al., 2009; Shi et al., 2021; Yigit and Christoforou, 2000). A series of complex vibrations such as drill string whirl motion, stick slip and high frequency torsional oscillation (HFTO) and their mitigation measures have been widely concerned (Kapitaniak et al., 2018; Navarro-López and Cortés, 2007; Oueslati et al., 2013; Tikhonov and Bukashkina, 2014; Tipples et al., 2021; Zhao et al., 2016). These studies of complex vibrations deepen the understanding of the dynamic characteristics of drill string and promotes the research level in vibration and control. In view of the ultra-slender characteristics of drill string and the strong nonlinear dynamic

* Corresponding author.
** Corresponding author.
*E-mail addresses:* chenfeng536@shu.edu.cn (F. Chen), qinfengd@shu.edu.cn (Q.-F. Di).
Peer review under the responsibility of China University of Petroleum (Beijing).

https://doi.org/10.1016/j.petsci.2025.05.026

characteristics, the numerical simulation method has a great advantage and has become one of the most important methods for studying the dynamic characteristics of drilling string in ultra-deep wells.

Among numerous numerical simulation methods, lumped mass models are often employed to represent the single degree of freedom structure (L'opez et al., 2004; Popp et al., 2003), and modally reduced models are often used to improve the computational efficiency (Khulief et al., 2007). The lumped mass models were effective in analyzing the dynamic characteristics of drill string, such as stick-slip and whirl motion, but it cannot fully reflect the vibration characteristics of drill string in borehole with complex spatial features. Therefore, researchers began to explore the finite element method (Dykstra, 1996; Khulief and Al-Naser, 2005) and multi-body dynamics method (Cheng et al., 2013; Wang et al., 2015) to study the dynamic characteristics of drill string, and have made important progress. Relatively speaking, the finite element method is rather common and successful in its application (Dykstra, 1996; Hu et al., 2012; Khulief and Al-Naser, 2005; Wang et al., 2024; Sivaram, 2023; Xi et al., 2023; Zhang et al., 2020; Zhu et al., 2008). Dykstra (1996) derived the finite element model of drill string dynamics based on the Hamilton principle, considering the geometric nonlinearity and contact nonlinearity of drill string, and calculated the dynamic characteristics of drill string with the combination of iterative method and Newmark method in view of the weak computer capability at that time. Khulief and Al-Naser (2005) presented a finite element model of the whole elastic drill string including both drill pipes and drill collars, which accounts for the axial-bending coupling, torsional-bending coupling, gyroscopic effect, gravitational stiffening effect and the associated tension and compression fields within the drill string. The model can be used to simulate stick-slip self-excited oscillation and to solve the transient vibration response of drill string due to different conditions. Zhu et al. (2008) established dynamics finite element model of drill string in the entire well, and studied the solution method of large nonlinear systems with uncertainty and dynamic boundary by using Wilson-$\theta$ step-by-step integral method. Hu et al. (2012) considered the initial curvature of the drill string, established the drill string dynamic finite element model based on the space curved beam element, developed the drill string dynamic simulation program, and realized the dynamic characteristics analysis of the drill string over 7000 m. The latest research results show that this method has been successfully applied to the well SDTK1, the first extra-deep well with a depth over 10,000 m in China (Wang et al., 2024).

It is no exaggeration to say that many researchers have carried out a lot of meaningful work in this field and achieved valuable research results, which greatly improved the dynamic safety of ultra-deep drilling string. However, the problem of drill string dynamic safety has not been well solved so far, and drill string failure accidents still occur frequently. One of the reasons for the above problems is that the current calculation method of drill string dynamics is not adapt to the complex working environment of drill string, and there is a deficiency in the optimization design methods for the structural parameters and drilling parameters of the drill string.

One of the fundamental causes underlying the aforementioned problems lies in the deficiency of effective calculation approaches. Although the works of Hu et al. (2012) and Zhang et al. (2020) have been able to simulate drill string dynamics and optimize parameters, the prolonged calculation time constrains the real-time performance of their works. It is commonly acknowledged that the key to calculate the drill string dynamic characteristics lies in the method of solving algebraic equations. Numerical solutions to algebraic equations typically include finite element method based on global matrix solution (Dykstra, 1996; Khulief and Al-Naser, 2005), boundary element method (Chen et al., 2022) and multi-body dynamics method (Cheng et al., 2013). And these can be divided into two categories: direct method and iteration method (Chen, 2020). The direct method refers to a methodology for obtaining the exact solution of equations through finite steps. It is often used to solve low-order dense matrix equations with high computational speed. Iteration method is one that acquires a relatively accurate solution through the process of step-by-step approximation, which requires less computing power and memory. It is suitable for solving problems with large sparse matrix equations, and computational efficiency is relatively low. The coefficient matrix of drill string mechanical model is a large sparse and ribbon shaped matrix, so it is more suitable to be solved by iteration method. Node iteration method only needs to carry out matrix operation between two units and three nodes and search nodes step by step, which has a good advantage in dealing with contact problems (Dykstra, 1996). However, the calculation time is prolonged and the calculation efficiency is poor due to multiple iterations over the entire range of drill string, which directly affects the application of this method.

The node iteration method acquires solution accuracy at the cost of time, and enhancing computational efficiency thus becomes its core aspect. At present, there are numerous iterative methods, such as the Jacobi iteration method, Gauss-Seidel iteration method, SOR iteration method, steepest descent method and conjugate gradient method, etc. (Li et al., 2008). SOR iteration method is a classical iteration method for solving linear equations, which is improved based on Gauss-Seidel iteration method. The concept is to modify the iterative formula through the weighted average approach in order to enhance the computational efficiency. The SOR iterative method converges more rapidly than the Jacobi iterative method, the Gauss-Seidel iterative method, and others, and the solution derived possesses higher accuracy. Therefore, it is widely applied in engineering practice (Wang, 2006).

In this paper, based on the node iteration method and in combination with the SOR iteration method, an accelerated calculation method for drill string dynamics, namely the SOR-node iteration method, is proposed. On the basis of the verification of the accuracy and validity of the solution program through numerical examples, the acceleration effect of this method in solving the dynamic characteristics of the drill string was analyzed, and the influence of the relaxation factor on the convergence rate of iteration was discussed. On this basis, a case of an extra-deep well was successfully solved by using the SOR node iteration method. Not only the calculation speed was significantly enhanced, but also the complex dynamic characteristics of the drill string in the extra-deep well were obtained.

## 2. Finite element model of drill string dynamics

When the drill string run into the narrow borehole filled with drilling fluid, its movement is not only influenced by the driving force of the ground rotary table and the excitation force from the drill bit-rock interaction, but also undergoes irregular collisions with the wellbore wall, resulting in a very complex stress state. The motion states of the drill string encompass axial vibration, lateral vibration, torsional vibration, as well as the mutual couplings among them.

### 2.1. Basic assumptions

When analyzing drill string dynamic characteristics, following assumptions are generally adopted (Khulief et al., 2005; Hu et al., 2012): (1) Deformation of drill string is small; (2) Drill string is regarded as a three-dimensional elastic beam element; (3) Borehole section is circular; (4) Influence of drill string joint is ignored; (5) Influence of shear strain caused by transverse force is ignored; (6) Influence of drilling fluid flow on drill string movement is ignored.

### 2.2. Coordinate system

In order to depict the motion of drill string in downhole, two coordinate system need to be established. One is the global coordinate system *OXYZ*: origin is in the center of the wellhead, *X* axis is vertically downward, *Y* axis points north, and *Z* axis points east, as shown in Fig. 1. And the other is the element coordinate system *oxyz*: origin is the element node, *x* axis is the tangent of the element axis at the node, directed towards the bottom of the well, *y* axis points to the high side of the hole, and *z* axis is determined by the right-hand rule, as shown in Fig. 2.

### 2.3. Equations of motion

A continuous drill string can be discretized into Euler-Bernoulli beam elements by finite element method. The drill string motion equation is given by Dykstra (1996).

$$\boldsymbol{M}\ddot{\boldsymbol{U}} + \boldsymbol{C}\dot{\boldsymbol{U}} + \boldsymbol{K}\boldsymbol{U} = \boldsymbol{F} \tag{1}$$

where $\boldsymbol{M}$ is the mass matrix; $\boldsymbol{C}$ is the damping matrix; $\boldsymbol{K}$ is the stiffness matrix; $\boldsymbol{F}$ is the external force matrix; $\ddot{\boldsymbol{U}}$, $\dot{\boldsymbol{U}}$, $\boldsymbol{U}$ are generalized acceleration, velocity and displacement vectors.

The mass matrix $\boldsymbol{M}$ consists of two parts, $\boldsymbol{M} = \boldsymbol{M}_1 + \boldsymbol{M}_2$, $\boldsymbol{M}_1$ contains the inertial mass of triaxial translation and rotation around the *x* axis, and $\boldsymbol{M}_2$ contains the inertial mass of rotation around *y* and *z* axes.

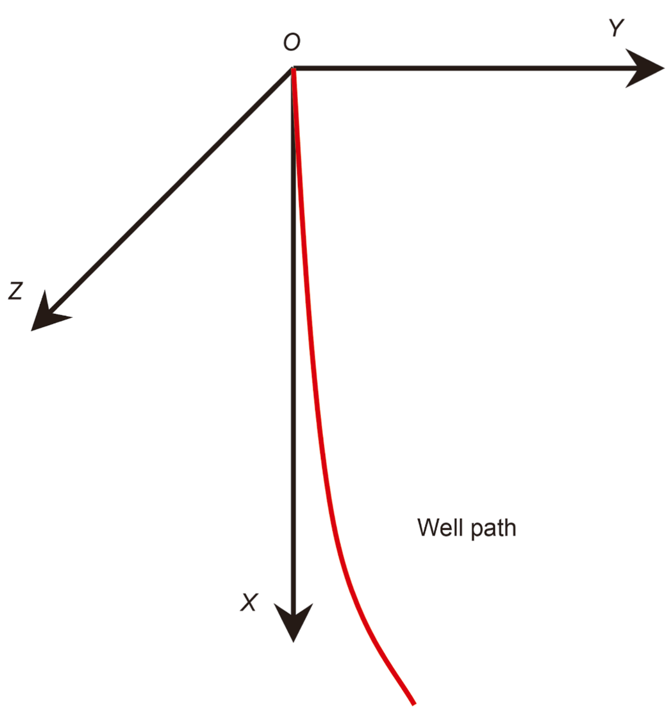

**Fig. 1.** Global coordinate system.

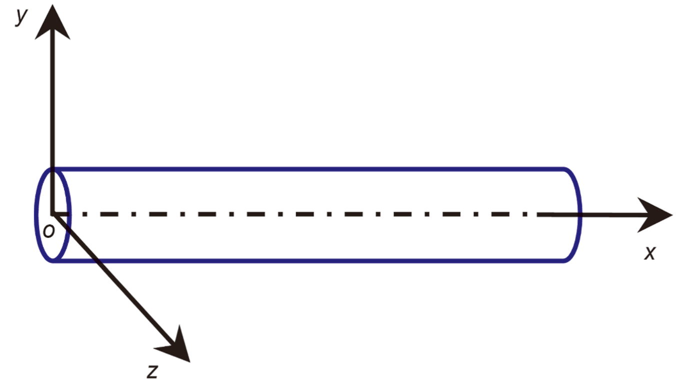

**Fig. 2.** Element coordinate system.

The damping matrix $\boldsymbol{C}$ of drill string motion is based on Rayleigh damping, and its expression is $\boldsymbol{C} = \alpha_r\boldsymbol{M} + \beta_r\boldsymbol{K}$, where $\alpha_r$ and $\beta_r$ are damping coefficients, which are determined by the inherent frequency of drill string system and the corresponding damping ratio.

The stiffness matrix $\boldsymbol{K}$ can be expressed as $\boldsymbol{K} = \boldsymbol{K}_\mathrm{l} + \boldsymbol{K}_\mathrm{n}$, where $\boldsymbol{K}_\mathrm{l}$ is a linear term and $\boldsymbol{K}_\mathrm{n}$ is a nonlinear term. $\boldsymbol{K}_\mathrm{n}$ can be divided into three parts, $\boldsymbol{K}_\mathrm{n} = \boldsymbol{K}_\mathrm{n1} + \boldsymbol{K}_\mathrm{n2} + \boldsymbol{K}_\mathrm{n3}$, where $\boldsymbol{K}_\mathrm{n1}$ represents the nonlinear stiffness matrix under the coupling effect of axial force and bending moment, $\boldsymbol{K}_\mathrm{n2}$ represents the nonlinear stiffness matrix under the coupling effect of axial force and torque, and $\boldsymbol{K}_\mathrm{n3}$ represents the nonlinear stiffness matrix under the coupling effect of torque and bending moment.

### 2.4. Boundary conditions and constraints

The transverse constraint of the drill string at the wellhead is regarded as a hinged support, and the axial direction is considered as a spring connection due to the effect of the hook. Meanwhile, the drill string at the wellhead is subjected to the output torque of the ground driving system. The lateral restraint at the drill bit is regarded as a hinged support, axially free, and is subjected to axial and torsional excitations resulting from the interaction between the drill bit and the formation. In addition, the drill string is constrained by the wellbore. When the lateral displacement of drill string exceeds the wellbore, it is considered that the drill string collided with the wellbore wall. At this point, the Hertz contact theory can be employed to establish the contact collision model, as shown in Fig. 3.

## 3. Solution method

### 3.1. Newmark-$\beta$ method

Newmark-$\beta$ method is a time integration algorithm based on discretizing the time domain for the study of dynamic problems. It converts the second-order differential equations of displacement with respect to time into algebraic equations of displacement at discrete time points (Qin et al., 2022).

The motion equation of drill string at any time $t$ is given by

$$\boldsymbol{M}\ddot{\boldsymbol{U}}_t + \boldsymbol{C}\dot{\boldsymbol{U}}_t + \boldsymbol{K}\boldsymbol{U}_t = \boldsymbol{F}_t \tag{2}$$

Newmark-$\beta$ method has following assumptions about velocity $\dot{\boldsymbol{U}}_{t+\Delta t}$ and displacement $\boldsymbol{U}_{t+\Delta t}$ at time $t+\Delta t$

$$\dot{\boldsymbol{U}}_{t+\Delta t} = \dot{\boldsymbol{U}}_t + \left[(1-\alpha)\ddot{\boldsymbol{U}}_t + \alpha\ddot{\boldsymbol{U}}_{t+\Delta t}\right]\Delta t \tag{3}$$

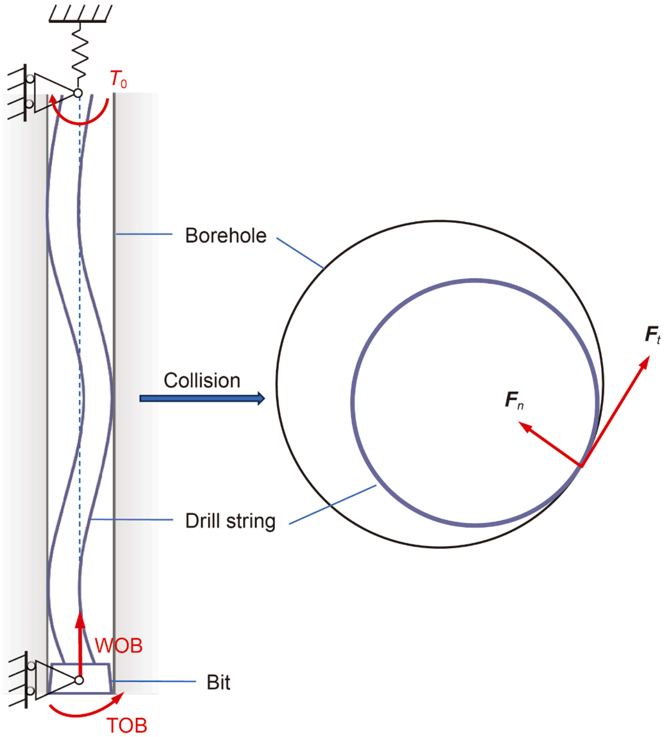


**Fig. 3.** Boundary conditions and constraints of drill string.

$$\boldsymbol{U}_{t+\Delta t} = \boldsymbol{U}_t + \dot{\boldsymbol{U}}_t\Delta t + \left[\left(\frac{1}{2}-\beta\right)\ddot{\boldsymbol{U}}_t + \beta\ddot{\boldsymbol{U}}_{t+\Delta t}\right]\Delta t^2 \tag{4}$$

where $\alpha$ and $\beta$ are the weight parameters. $\dot{\boldsymbol{U}}_{t+\Delta t}$ and $\ddot{\boldsymbol{U}}_{t+\Delta t}$ can be obtained by Eqs. (5) and (6)

$$\ddot{\boldsymbol{U}}_{t+\Delta t} = \frac{1}{\beta\Delta t^2}(\boldsymbol{U}_{t+\Delta t} - \boldsymbol{U}_t) - \frac{1}{\beta\Delta t}\dot{\boldsymbol{U}}_t - \left(\frac{1}{2\beta}-1\right)\ddot{\boldsymbol{U}}_t \tag{5}$$

$$\dot{\boldsymbol{U}}_{t+\Delta t} = \frac{\alpha}{\beta\Delta t}(\boldsymbol{U}_{t+\Delta t} - \boldsymbol{U}_t) - \left(\frac{\alpha}{\beta}-1\right)\dot{\boldsymbol{U}}_t - \left(\frac{\alpha}{2\beta}-1\right)\ddot{\boldsymbol{U}}_t\Delta t \tag{6}$$

Substitute Eqs. (5) and (6) into Eq. (2) yields

$$\begin{aligned}(\lambda_1\boldsymbol{M} + \lambda_4\boldsymbol{C} + \boldsymbol{K})\boldsymbol{U}_{t+\Delta t} = \boldsymbol{F}_{t+\Delta t} + \boldsymbol{M}\left(\lambda_1\boldsymbol{U}_t + \lambda_2\dot{\boldsymbol{U}}_t + \lambda_3\ddot{\boldsymbol{U}}_t\right)\\ +\boldsymbol{C}\left(\lambda_4\boldsymbol{U}_t + \lambda_5\dot{\boldsymbol{U}}_t + \lambda_6\ddot{\boldsymbol{U}}_t\right)\end{aligned} \tag{7}$$

where $\lambda_1 = \frac{1}{\beta\Delta t^2}$, $\lambda_2 = \frac{1}{\beta\Delta t}$, $\lambda_3 = \frac{1}{2\beta} - 1$, $\lambda_4 = \frac{\alpha}{\beta\Delta t}$, $\lambda_5 = \frac{\alpha}{\beta} - 1$, $\lambda_6 = \left(\frac{\alpha}{2\beta} - 1\right)\Delta t$.

Based on the displacement $\boldsymbol{U}_t$, velocity $\dot{\boldsymbol{U}}_t$, acceleration $\ddot{\boldsymbol{U}}_t$ at time $t$ and the external force vector $\boldsymbol{F}_{t+\Delta t}$ at time $t+\Delta t$, the displacement $\boldsymbol{U}_{t+\Delta t}$ at time $t+\Delta t$ can be obtained, and then the velocity $\dot{\boldsymbol{U}}_{t+\Delta t}$ and acceleration $\ddot{\boldsymbol{U}}_{t+\Delta t}$ can be derived. Therefore, the motion state at any time can be obtained from the initial configuration.

### 3.2. Node iteration method

After discretizing the time domain by the Newmark method, the displacement at each moment is solved by using the node iteration method. The flowchart of the node iteration method is shown in Fig. 4.

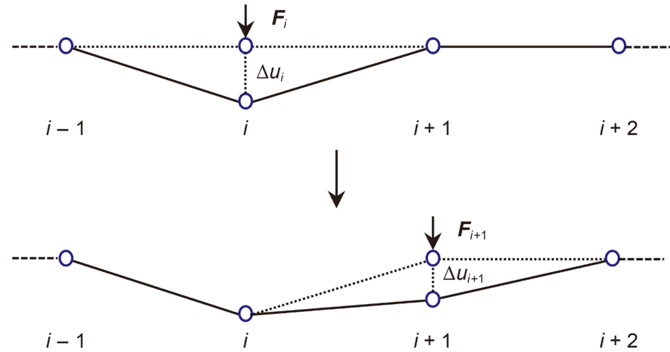


**Fig. 4.** Node iteration method.

Node iteration method takes three nodes of two elements as the minimum computing unit. Assuming that the displacement of node $i-1$ and $i+1$ is given, the displacement of node $i$ can be calculated according to the principle of local mechanical equilibrium, and then the displacement of node $i+1$ can be calculated from the displacement of node $i$ and $i+2$. The equilibrium equation regarding the node $i$ can be represented as

$$\boldsymbol{F}_i = \begin{bmatrix}\boldsymbol{K}_{i,i-1} & \boldsymbol{K}_{i,i} & \boldsymbol{K}_{i,i+1}\end{bmatrix}\begin{bmatrix}\boldsymbol{U}_{i-1} & \boldsymbol{U}_i & \boldsymbol{U}_{i+1}\end{bmatrix}^T \tag{8}$$

The displacement of node $i$ can be written by

$$\boldsymbol{U}_i = \boldsymbol{K}_{i,i}^{-1}\left[\boldsymbol{F}_i - \left(\boldsymbol{K}_{i,i-1}\boldsymbol{U}_{i-1} + \boldsymbol{K}_{i,i+1}\boldsymbol{U}_{i+1}\right)\right] \tag{9}$$

Upon obtaining the displacement of node $i$, it is requisite to judge whether this node is contact with the wellbore wall. If contact, the corresponding contact force and contact moment based on the Hertz contact model (Christoforou and Yigit, 1997) are added to the external force vector $\boldsymbol{F}_i$ at this node, so as to guarantee that the drill string is located within the wellbore wall at the node. Starting from the top of the drill string and computing all nodes to the bottom of the drill string, and then from the bottom to the top, one iteration step is accomplished. After a finite number of iterations, the result tends to stabilize, and at this point, the overall configuration of the drill string is determined.

## 4. Methods for speeding up calculations and its verification

### 4.1. SOR node iteration method

Through years of efforts, Hu et al. (2011) successfully realized the simulation of dynamic characteristics of drill string over 7000 m long by using node iteration method, which was well applied to dynamic safety evaluation of drill string and the optimization design of operating parameters in ultra-deep wells of Tarim Oilfield, China. However, node iteration is a process of gradually approaching the exact solution, and its convergence rate will decrease with the increase of the number of iterations. For the 7000 m ultra-long drill string, the iterative calculation time on the Matlab programming language platform of the high-performance computer (with the processor Intel Xeon Gold 6330 at 2.00 GHz and a memory of 256 G) approaches 8 h. Therefore, it is urgent to find an iteration acceleration method to improve the computational efficiency while ensuring the accuracy. In this paper, the successive over relaxation (SOR) iterative method is employed to enhance the calculation speed.

It can be seen from Section 3 that the key to obtain the dynamic response of drill string over a period of time is to solve algebraic

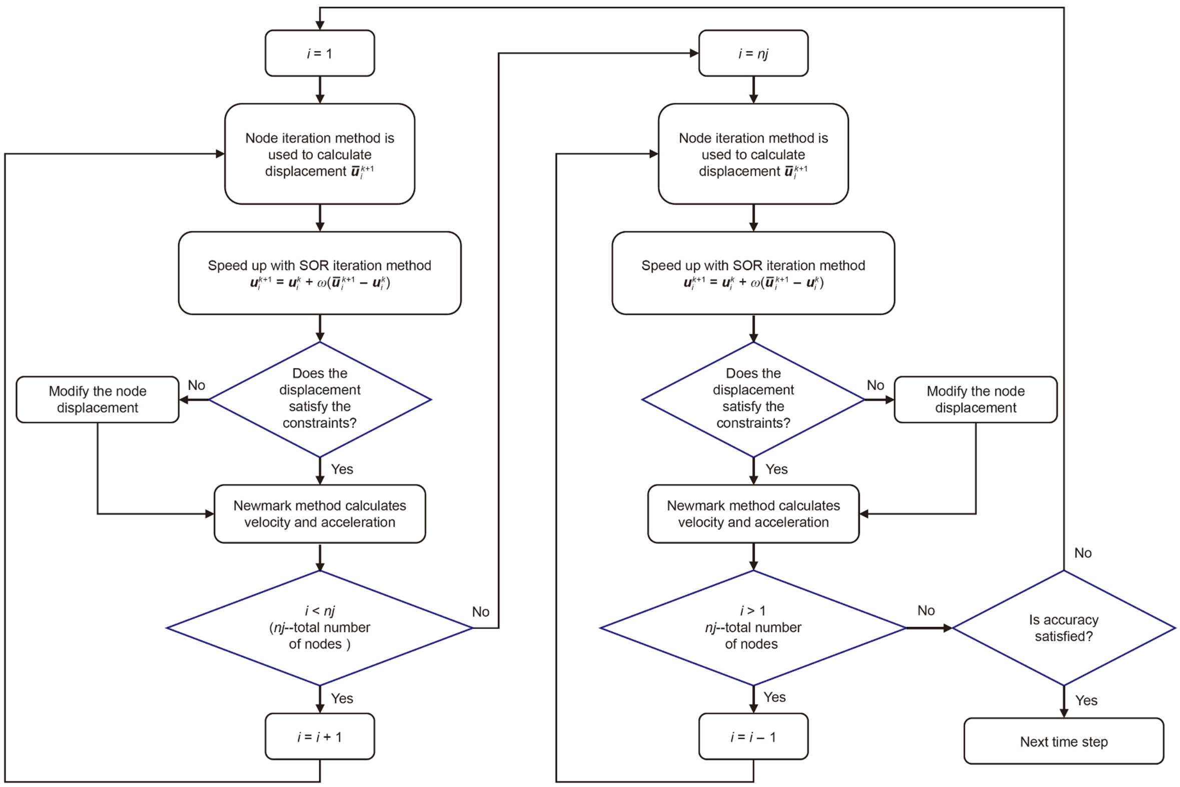


**Fig. 5.** Calculation flow chart of SOR node iteration method.

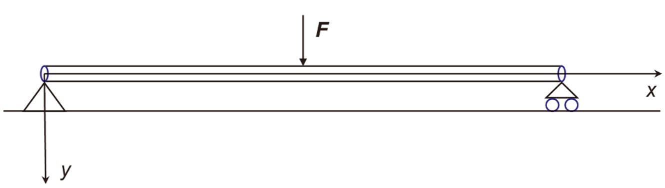


**Fig. 6.** Simply supported beam model.

equations of displacement at the time discrete points. At time $t + \Delta t$, Eq. (7) can be written as

$$\tilde{\boldsymbol{K}}_{t+\Delta t}\boldsymbol{U}_{t+\Delta t} = \tilde{\boldsymbol{F}}_{t+\Delta t} \tag{10}$$

where $\tilde{\boldsymbol{K}}_{t+\Delta t}$ is the equivalent stiffness matrix, $\tilde{\boldsymbol{F}}_{t+\Delta t}$ is the equivalent force matrix, and can be expressed as

$$\tilde{\boldsymbol{K}}_{t+\Delta t} = \lambda_1\boldsymbol{M} + \lambda_4\boldsymbol{C} + \boldsymbol{K} \tag{11}$$

$$\tilde{\boldsymbol{F}}_{t+\Delta t} = \boldsymbol{F}_{t+\Delta t} + \boldsymbol{M}\left(\lambda_1\boldsymbol{U}_t + \lambda_2\dot{\boldsymbol{U}}_t + \lambda_3\ddot{\boldsymbol{U}}_t\right) + \boldsymbol{C}\left(\lambda_4\boldsymbol{U}_t + \lambda_5\dot{\boldsymbol{U}}_t + \lambda_6\ddot{\boldsymbol{U}}_t\right) \tag{12}$$

Thus, Eq. (10) can be regarded as a system of linear equations of the form $\boldsymbol{Au} = \boldsymbol{b}$. In the drill string mechanics model, $\boldsymbol{A}$ is a large sparse matrix with nonzero elements distributed in a ribbon along the main diagonal of the matrix. In view of the large number of zero elements in matrix $\boldsymbol{A}$, node iteration method can reduce the memory consumption of computer. The mathematical essence of node iteration method is Gauss-Seidel iteration method. SOR iteration method is an improved method of Gauss-Seidel iteration method, adding relaxation factor $\omega$ to accelerate the convergence speed of iteration calculation (Hu and Yu, 2006).

For the linear equation system $\boldsymbol{Au} = \boldsymbol{b}$, it is assumed that the vector $\boldsymbol{u}_i^{(k)}(i = 1, 2, \ldots, nj)$ of the $k$-th iteration and the vector component $\boldsymbol{u}_j^{(k+1)}(j = 1, 2, \ldots, i-1)$ of the $(k+1)$-th iteration are known. The vector component $\boldsymbol{u}_i^{(k+1)}$ can be obtained by following two steps:

(1) The auxiliary quantity $\bar{\boldsymbol{u}}_i^{(k+1)}$ is defined by Gauss-Seidel iteration method

$$\bar{\boldsymbol{u}}_i^{(k+1)} = \frac{1}{a_{ii}}\left(b_i - \sum_{j=1}^{i-1} a_{ij}\boldsymbol{u}_j^{(k+1)} - \sum_{j=i+1}^{n} a_{ij}\boldsymbol{u}_j^{(k)}\right) \tag{13}$$

where $a_{ii}$ and $a_{ij}$ are corresponding elements in coefficient matrix $\boldsymbol{A}$, $b_i$ is corresponding element in matrix $\boldsymbol{b}$.

(2) Then $\boldsymbol{u}_i^{(k+1)}$ is defined by weighted average of $\boldsymbol{u}_i^{(k)}$ and $\bar{\boldsymbol{u}}_i^{(k+1)}$

**Table 1**
Parameters of simply supported beam.

| Total length, m | Element length, m | Outside diameter, m | Inside diameter, m | Density, kg/m$^3$ | Elasticity modulus, Pa | $\boldsymbol{F}$, kN |
|---|---|---|---|---|---|---|
| 20 | 1 | 0.203 | 0.076 | $7.85 \times 10^3$ | $201 \times 10^9$ | 10 |

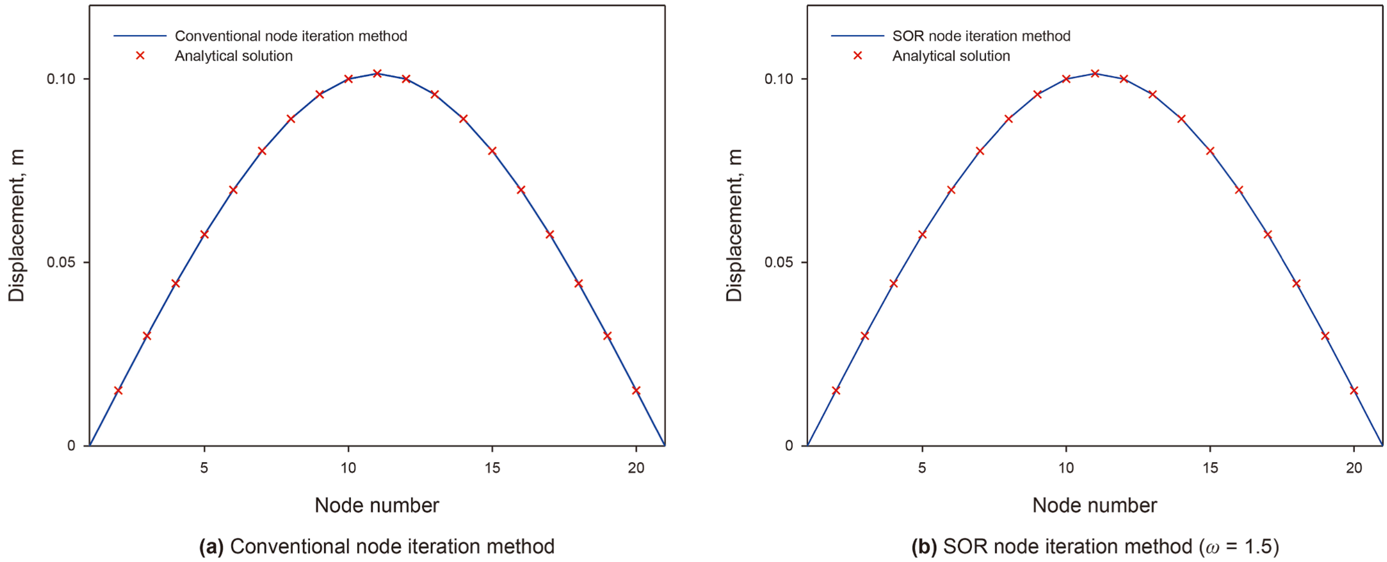


**Fig. 7.** Comparison of calculation results of two kinds of iteration methods.

**Table 2**
Iterations and time used in each iteration method.

| Method | Iterations | Time, s |
|---|---|---|
| Conventional node iteration method | 149,560 | 81.566 |
| SOR node iteration method ($\omega = 1.5$) | 99,904 | 53.467 |

$$\boldsymbol{u}_i^{(k+1)} = \boldsymbol{u}_i^{(k)} + \omega\left(\overline{\boldsymbol{u}}_i^{(k+1)} - \boldsymbol{u}_i^{(k)}\right) \tag{14}$$

where $\omega$ is the relaxation factor, $0<\omega<2$. In case of $0< \omega< 1$, the above equation is called low relaxation iteration method. In case of $\omega = 1$, the above equation is called Gauss-Seidel iteration method. In case of $1 \leq \omega<2$, the above equation is called over relaxation iteration method. This paper studies the case of $1 \leq \omega< 2$. The proof of convergence of SOR iteration method can be referred to (Xu, 2002). The flow chart of SOR node iteration method is shown in Fig. 5.

### 4.2. Validation of SOR node iteration method

Taking a simply supported beam placed horizontally as an example, and the force $\boldsymbol{F}$ acts on the midpoint of the beam (as shown in Fig. 6). The relevant parameters are presented in Table 1. Conventional node iteration method and SOR node iteration method are used for calculation respectively. Iteration accuracy is set as $\delta = 10^{-9}$, and relaxation factor of SOR node iteration method is set as $\omega = 1.5$. The calculation results are shown in Fig. 7.

According to the theory of material mechanics, the analytical solution of the simply supported beam is

$$\begin{cases} y = \dfrac{\boldsymbol{F}x}{12EI}\left(\dfrac{3l^2}{4} - x^2\right) & 0 \leq x \leq \dfrac{l}{2} \\ y = \dfrac{\boldsymbol{F}}{12EI}\left(x^3 - 3lx^2 + \dfrac{9l^2}{4}x - \dfrac{l^3}{4}\right) & \dfrac{l}{2} \leq x \leq l \end{cases} \tag{15}$$

And $y_{\max} = \frac{Fl^3}{48EI}$, maximum deflection of given simply supported beam is 0.101465 m. The result obtained by SOR node iteration method and conventional node iteration method is the same as 0.101448 m, with an error of 0.02%. As can be seen from Table 2, when $\omega = 1.5$, the number of iterations of SOR node iteration method is reduced by 33.2% and the calculation time is reduced by 34.4% compared with conventional node iteration method. The accuracy of SOR node iteration method is verified by the simple supported beam example, and it has a good effect on speeding up the calculation.

## 5. Case study

### 5.1. Speed up effect of SOR node iteration method

The drill string assembly of a certain extra-deep well in the western region of China is as follows: 241.3 mm PDC bit ×

**Table 3**
Comparison of computational efficiency.

| Method | Iterations | Time, s |
|---|---|---|
| Conventional node iteration method | 2,107,589 | 141,483 |
| SOR node iteration method ($\omega = 1.9$) | 1,118,801 | 73,253 |

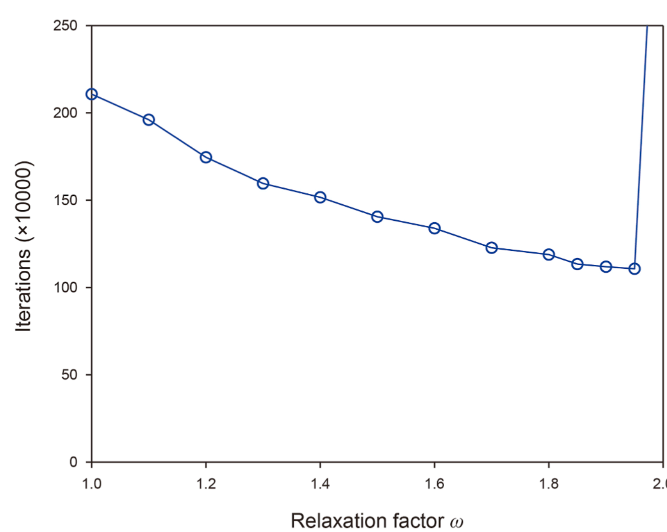


**Fig. 8.** Relationship between relaxation factor and iterations.

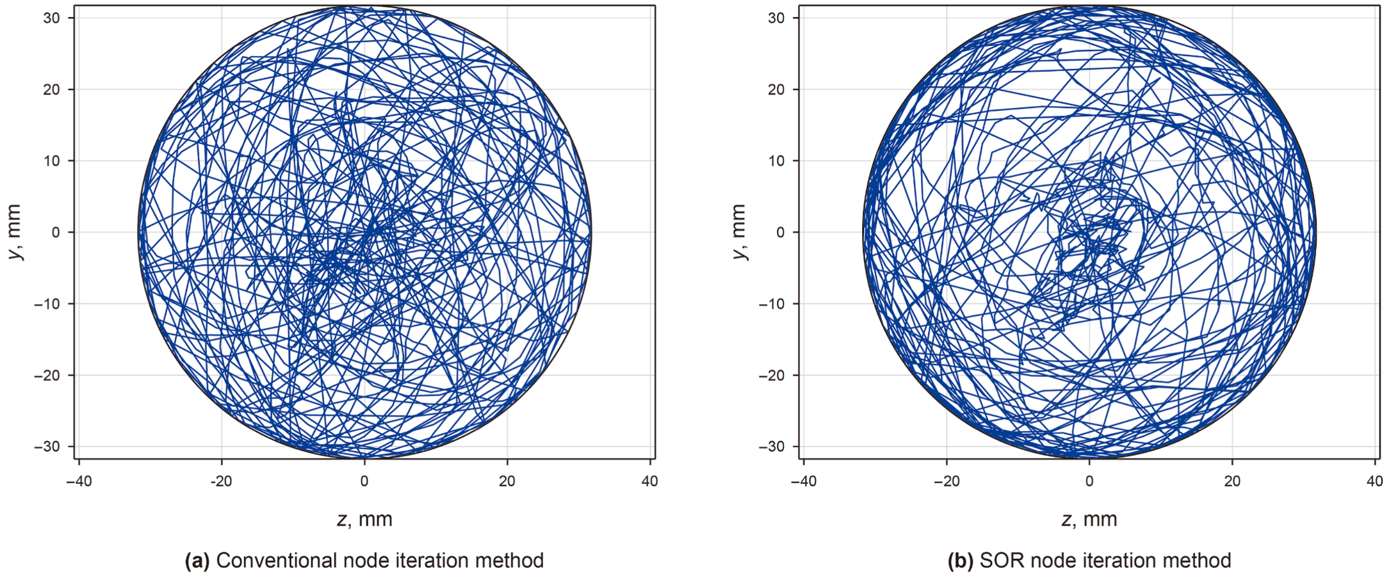


**Fig. 9.** Whirl trajectory of drill string centroid at midpoint between the bit and the lower stabilizer.

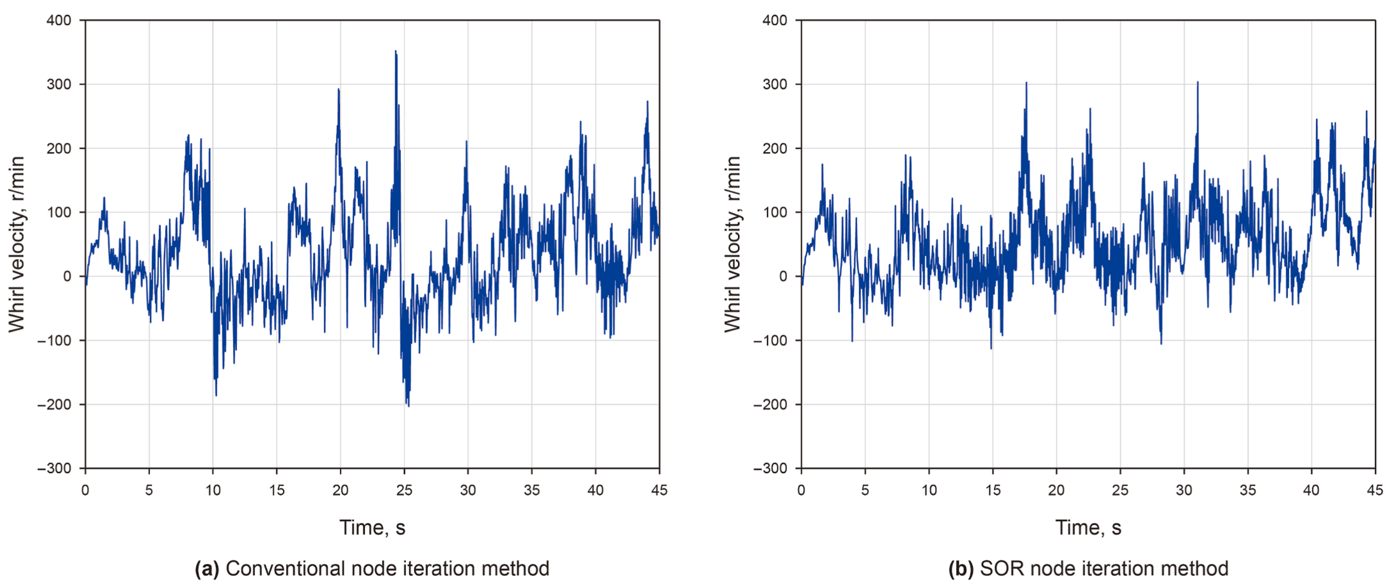


**Fig. 10.** Whirl velocity of drill string centroid at midpoint between the bit and the lower stabilizer.

0.30 m + 177.8 mm (71.4 mm) drill collar × 18.00 m + 241 mm stabilizer (71.4 mm) × 1.80 m + 177.8 mm (71.4 mm) drill collar × 9.00 m + 241 mm (71.4 mm) stabilizer × 1.80 m + 177.8 mm (71.4 mm) drill collar × 123.00 m + 139.7 mm (92.1 mm) heavy weighted drill pipe × 142.00 m + 139.7 mm (121.4 mm) drill pipe × 3400.00 m + 149.3 mm (129.9 mm) drill pipe × 5707.00 m. The inside diameter of the drill string is shown in brackets, and the total length of drill string is 9402.90 m.

In addition, surface rotational speed is 90 r/min, weight on bit is 120 kN, drilling fluid density is 1800 kg/m$^3$, and borehole inclination is 0.5°. Newmark parameter $\alpha$ is 0.5 and $\beta$ is 0.25. Calculate the dynamics of drill string within 45 s, with a single step interval of 0.02 s. Iteration accuracy is set as $\delta = 10^{-6}$. Relaxation factor $\omega = 1.9$.

Table 3 lists iterations and time of SOR node iteration method and conventional node iteration method. Conventional node iteration method has 2,107,589 iterations and takes 141,483 s. Compared with conventional node iteration method, SOR node iteration method reduces the number of iterations by 46.9% and the time by 48.2%.

In fact, the value of relaxation factor $\omega$, is the key to affect speed and stability of iteration convergence, and it is very important to select the appropriate relaxation factor. How to choose an appropriate relaxation factor is a challenging problem. The optimal relaxation factor may vary with matrix structure, iteration initial value and boundary conditions. The convergence speed and stability of the calculation were observed by selecting different relaxation factors.

The number of iterations corresponding to different relaxation factor $\omega$ is shown in Fig. 8. With the increasing of $\omega$, the number of iterations decreases gradually. When $\omega$ takes 1.9, the number of iterations and the time for achieving calculation stability are at a

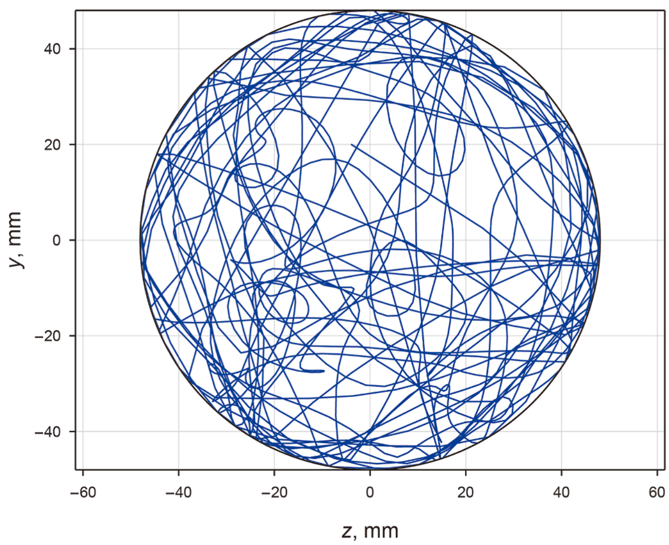


**Fig. 11.** Whirl trajectory of drill string centroid at position B.

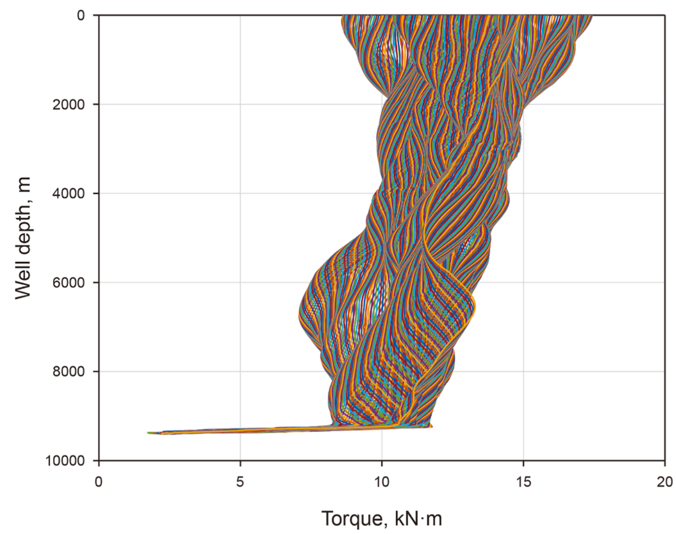


**Fig. 13.** Dynamic torque of the extra-deep well drill string.

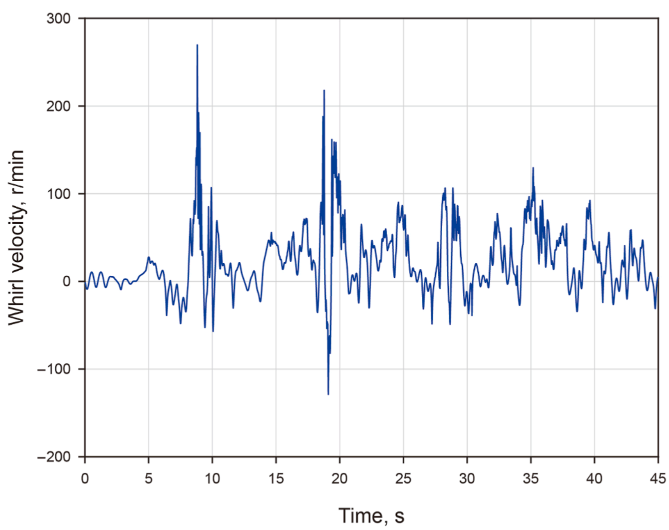


**Fig. 12.** Whirl velocity of drill string centroid at position B.

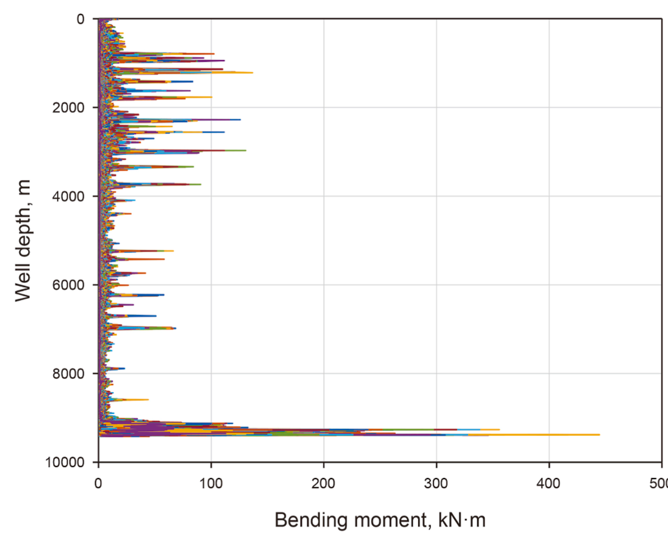


**Fig. 14.** Dynamic bending moment of the extra-deep well drill string.

minimum. When $\omega$ approaches 2, the number of iterations increases sharply. Relaxation factor $\omega$ determines the weight ratio of new and old solutions for each iteration. When $\omega$ approaches 2, the proportion of new solutions is too large, that is, the amplitude of each iteration update is too large, which may cause the iteration process to fluctuate back and forth in different directions, resulting in poor iteration convergence or even divergence.

### 5.2. Numerical results

Figs. 9 and 10 present the whirl trajectory and whirl velocity of drill string centroid at the midpoint between the bit and the lower stabilizer (depth 9392.60 m), which are calculated by SOR node iteration method and conventional node iteration method.

The results of two methods are basically consistent. Examination of the details reveals that the whirl trajectory calculated by the traditional node iteration method collide relatively more with the wellbore, and consequently, the fluctuations in whirl velocity occur more frequently compared to those calculated by the SOR node iteration method. The fluctuation range of whirl velocity obtained by conventional node iteration method is −203.1 to 352.1 r/min, with an average value of 33.5 r/min. And the fluctuation range of whirl velocity obtained by SOR node iteration method is −112.9 to 303.6 r/min, with an average value of 54.3 r/min. The principal fluctuation intervals of the whirl velocity derived from the two methods are both within −100 to 200 r/min.

Figs. 11 and 12 show the whirl trajectory and velocity of drill string centroid at midpoint of drill string (depth 4700.51 m). The fluctuation range of whirl velocity obtained by SOR node iteration is −128.7 to 269.5 r/min, with an average value of 23.7 r/min. The forward and backward whirls of drill string at this position are irregularly alternating, which basically reflects motion characteristics of the midpoint of drill string in vertical well.

The overall dynamic torque of the extra-deep well drill string varies with time as illustrated in Fig. 13, the curves of different colors in the figure stand for different moments. It can be observed that the dynamic torque increases rapidly at the position of the bottom stabilizer, indicated that the frictional torque at the stabilizer has a significant influence on the overall torque.

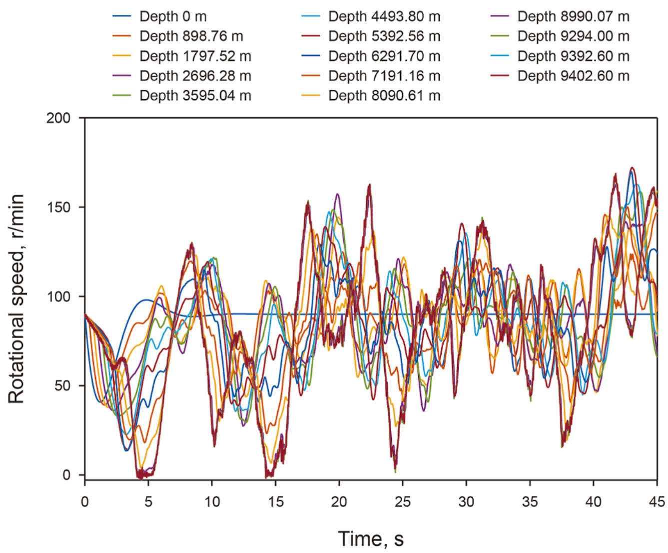


**Fig. 15.** Rotational speed of drill string at different well depths.

The dynamic bending moment of the entire well drill string is presented in Fig. 14. As the outer diameter of the bottom stabilizer is relatively large, its connection with the drill collar formed a variable cross-section structure, giving rise to a considerable change in the bending moment at the sections of the stabilizer.

Fig. 15 presents the variations of rotational speed of drill string at different well depths. It can be observed from the figure that the speed tends to stabilize after 10 s, and the trend of rotational speed change in the lower section is essentially in accordance with that in the upper section. However, in the vicinity of the drill bit, the rotational speed of the drill string fluctuates extremely vigorously, with the minimum rotational speed approximating 0.0 r/min and the maximum rotational speed approaching 170.0 r/min. Namely, the drill string might generate a stick-slip torsional vibration of stick-slip in the downhole.

To represent the lateral vibration status of the extra-deep well drill string clearly, three positions, close to the wellhead (depth 8.99 m), the midpoint of the drill string (depth 4700.51 m), and near the bottom (depth 9392.60 m) of the well, are selected for comparison of their lateral vibration amplitudes and frequencies, as presented in Figs. 16 and 17. It can be observed from the figures that among the three positions, the lateral vibration amplitude at the midpoint of the drill string is the largest, that near the bottom of the well takes the second place, while the lateral vibration amplitude near the wellhead at the upper part is the smallest. This is because the constraints at the wellhead, the bottom of the well, and the stabilizer, along with the coupling effect of large axial forces, have restricted the fluctuations of lateral displacement. It can be inferred from the spectral curves of the $y$-direction displacement of the three positions in Fig. 17 that the vibration frequency at the midpoint of the drill string is relatively low and the vibration amplitude is relatively large. The reason lies in the fact that the position is far removed from the constraints at both ends. Compared with the position close to the wellhead, the vibration frequency of the drill string near the bottom of the well is similar, yet the vibration intensity is higher, suggesting that the vibrations in the lower part are more intense. The overall tendency of the frequency distribution in the $z$-direction is analogous to that in the $y$-direction. However, at the midpoint of the entire well, the vibration intensity in the $z$-direction within the 0–2 Hz range is conspicuously lower than that in the $y$-direction, suggesting that the vibrations of the drill string in the two orthogonal lateral directions are not homogeneous and might be affected by the well trajectory, moving in the area close to the direction of lower shaft wall.

The lateral vibration characteristics of the entire well drill string are depicted in Fig. 18. It can be conspicuously observed that when the calculation becomes stable (approximately 10 s later), the lateral vibrations in the middle and lower parts of the drill string are significant (with alternating deep red and deep blue spots and larger spot areas). However, at the uppermost and lowermost parts, the amplitude of the lateral vibration of the drill string is smaller and the frequency is higher. This is manifested in the graph as an increased density of the spots and a reduced color contrast. This is attributed to the fact that the upper part of the extra-deep well drill string is subjected to a considerable axial tensile force, under the straightening effect, its lateral movement is reduced but the frequency increases. Meanwhile, the lower part of the BHA has its lateral displacement restricted by the double stabilizers, additionally, the drill collar has a larger diameter and a smaller gap with the wellbore, making it more susceptible to micro-amplitude and high-frequency vibrations.

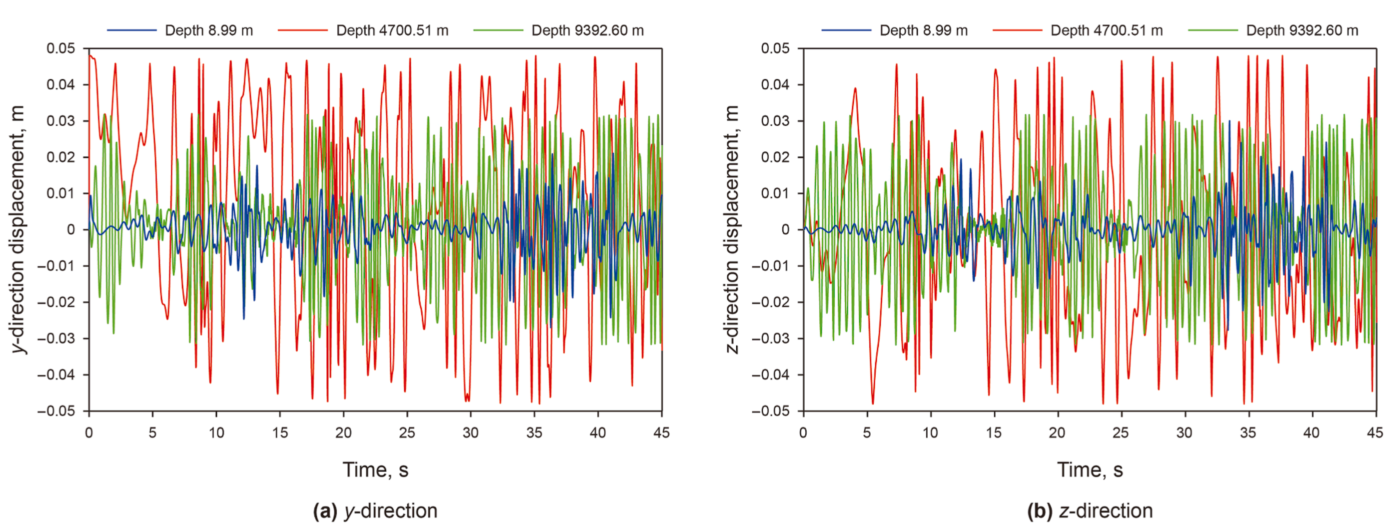


**Fig. 16.** The lateral vibration amplitudes at different position of drill string.

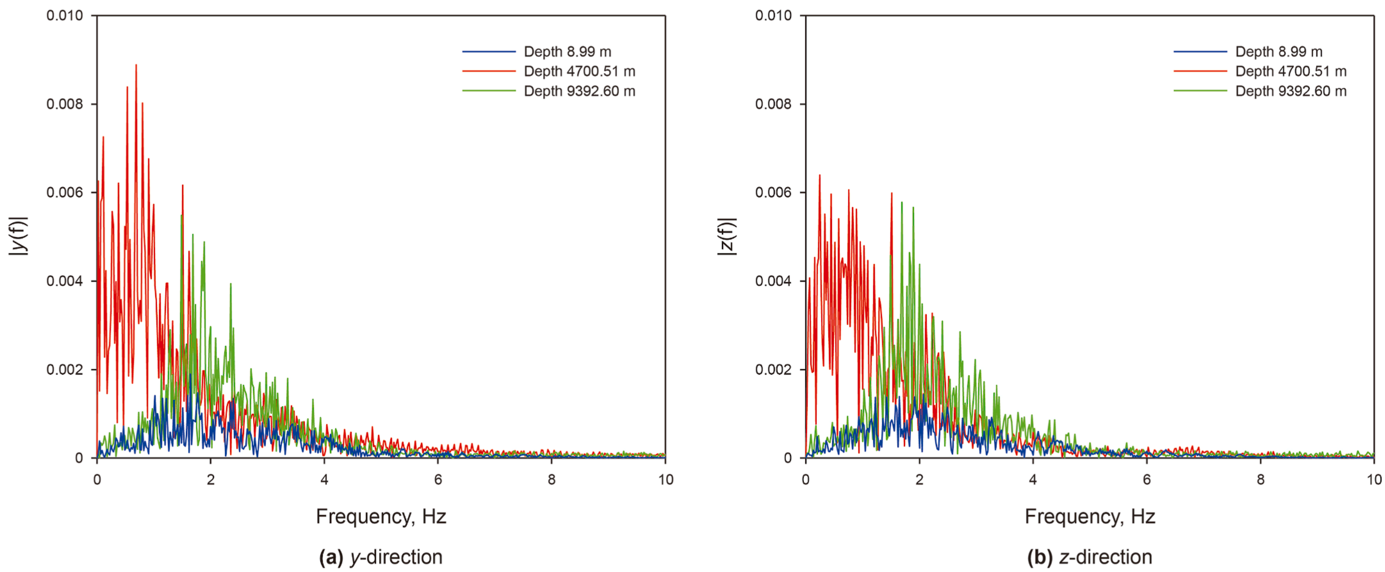


**Fig. 17.** The lateral vibration frequencies at different position of drill string.

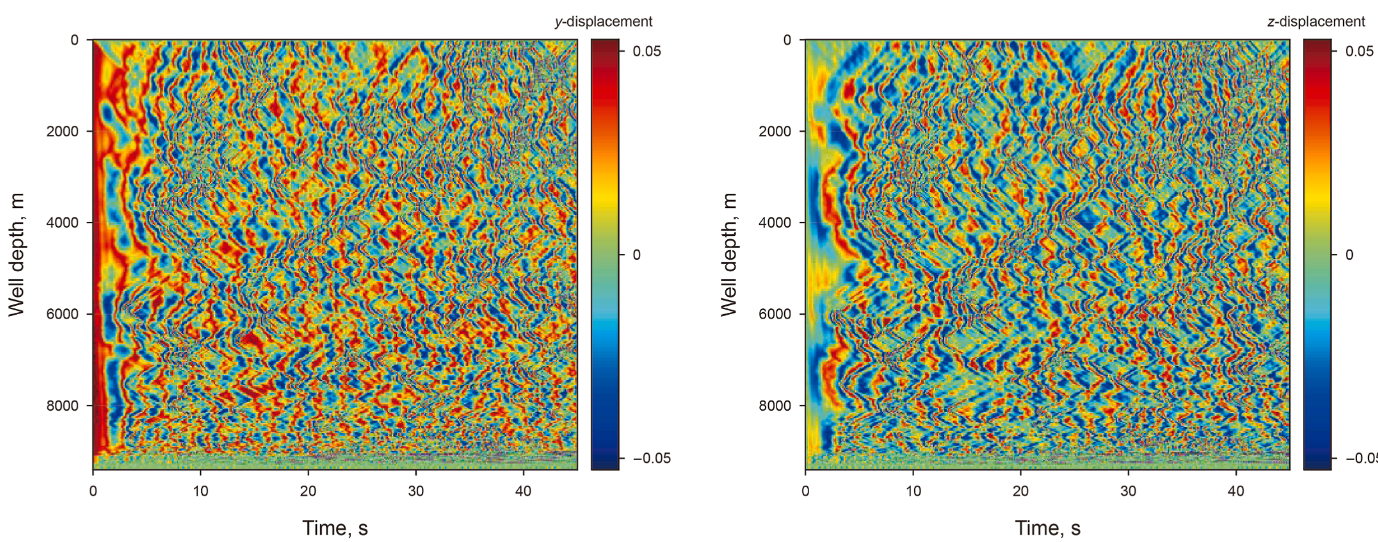


**Fig. 18.** The lateral vibration characteristics of the entire well drill string.

## 6. Conclusions

The computational efficiency is crucial for grasping the motion state of the drill string in extra-deep well. In this paper, SOR node iteration method was proposed to accelerate the calculation speed, and the dynamic characteristics of the drill string in extra-deep well were calculated through this method. Conclusions are as follows.

(1) The dynamic characteristics of extra-deep well drill strings are extremely complex, numerical solutions are highly time-consuming. Based on the SOR node iteration method, the dynamic characteristics simulation of extra-deep well drill string can be achieved, and the speed is increased by 48.2% compared with the traditional node iteration method.

(2) The violent vibration of the drill string for extra-deep wells is attributed to the super slenderness ratio and strong nonlinearity. The rotational speed fluctuations at different positions of the drill string intensify with the increase in depth. Near the drill bit, a stick-slip vibration is prone to occur. The dynamic torque and dynamic bending moment of the bottom drill string are conspicuously influenced by the stabilizers. The lateral vibration intensities in the middle and lower parts of the drill string are relatively large, while the lateral vibration frequencies of the upper and bottom parts of drill string are more intricate.

(3) The SOR node iteration method is capable of effectively accelerating the convergence rate of iterations and enhancing computational efficiency. The influence of the relaxation factor on the speed-up effect of the SOR node iteration method is quite remarkable. For extra-deep well drill strings, with the increase of the relaxation factor, the number of iterations gradually reduces. When the relaxation factor takes the value of 1.9, the number of iterations reaches the minimum and then increases rapidly.

(4) The dynamic characteristics of the drill string in extra-deep wells are subject to multiple factors, such as wellbore trajectory, formation features, drill string structure, and drilling parameters. Although this paper has not delved into the influence of these factors on the dynamic characteristics of the drill string in extra-deep wells and the control mechanisms of these parameter in detail, the proposed SOR node iteration method has remarkably improved the computational efficiency of the dynamic characteristics of the drill string in extra-deep wells. This advancement offers substantial support for the subsequent studies related to the influence of parameters.

## CRediT authorship contribution statement

**Wen-Chang Wang:** Writing – original draft, Formal analysis, Conceptualization. **He-Yuan Yang:** Data curation. **Da-Kun Luo:** Formal analysis. **Ming-Ming You:** Methodology. **Xing Zhou:** Visualization. **Feng Chen:** Writing – review & editing, Supervision. **Qin-Feng Di:** Writing – review & editing, Supervision, Project administration.

## Declaration of competing interest

The authors declare that they have no known competing financial interests or personal relationships that could have appeared to influence the work reported in this paper.

## Acknowledgments

This research was supported by the National Natural Science Foundation of China (52174003, 52374008).

## References

Chen, L.J., 2020. Calculation Method. Beijing. Beijing Institute of Technology Press, pp. 69–110 (in Chinese).
Chen, M., Guo, T.K., Qu, Z.Q., et al., 2022. Numerical investigation into hydraulic fracture initiation and breakdown pressures considering wellbore compliance based on the boundary element method. J. Petrol. Sci. Eng. 211, 110162. https://doi.org/10.1016/j.petrol.2022.110162.
Cheng, Z.B., Jiang, W., Ren, G.X., et al., 2013. A multibody dynamical model for full hole drillstring dynamics. Appl. Mech. Mater. 378, 91–96. https://doi.org/10.4028/www.scientific.net/AMM.378.91.
Christoforou, A.P., Yigit, A.S., 1997. Dynamic modelling of rotating drillstrings with borehole interactions. J. Sound Vib. 206 (2), 243–260. https://doi.org/10.1006/jsvi.1997.1091.
Dykstra, M.W., 1996. Nonlinear Drill String Dynamics. Doctoral dissertation. The University of Tulsa.
Hu, F., Yu, F.X., 2006. Overrelaxation iteration method in the selection of relaxation factor omega method. Journal of Qinghai Normal University (science edition) (1), 42–45. https://doi.org/10.16229/j.cnki.issn1001-7542.2006.01.013 (in Chines).
Hu, Y.B., 2011. Finite Element Analysis of Dynamic Characteristics of Drillstring Based on Actual Well Path. Doctoral Dissertation. Shanghai University (in Chinese).
Hu, Y.B., Di, Q.F., Zhu, W.P., et al., 2012. Dynamic characteristics analysis of drillstring in the ultra-deep well with spatial curved beam finite element. J. Petrol. Sci. Eng. 82–83, 166–173. https://doi.org/10.1016/j.petrol.2012.01.011.
Kapitaniak, M., Vaziri, V., Chávez, J.P., et al., 2018. Experimental studies of forward and backward whirls of drill-string. Mech. Syst. Signal Process. 100, 454–465. https://doi.org/10.1016/j.ymssp.2017.07.014.
Khulief, Y.A., Al-Naser, H., 2005. Finite element dynamic analysis of drillstrings. Finite Elem. Anal. Des. 41 (13), 1270–1288. https://doi.org/10.1016/j.finel.2005.02.003.
Khulief, Y.A., Al-Sulaiman, F.A., Bashmal, S., 2007. Vibration analysis of drillstrings with self-excited stick–slip oscillations. J. Sound Vib. 299, 540–558. https://doi.org/10.1016/j.jsv.2006.06.065.
Li, Q.Y., Wang, N.C., Yi, D.Y., 2008. Numerical Analysis. Tsinghua University Press, Beijing, pp. 193–197 (in Chinese).
López, I., Busturia, J.M., Nijmeijer, H., 2004. Energy dissipation of a friction damper. J. Sound Vib. 278 (3), 539–561. https://doi.org/10.1016/j.jsv.2003.10.051.
Moraes, L.P., Savi, M.A., 2018. Drill-string vibration analysis considering an axial-torsional-lateral non-smooth model. J. Sound Vib. 438, 220–237. https://doi.org/10.1016/j.jsv.2018.08.054.
Naganawa, S., 2012. Feasibility study on roller-cone bit wear detection from axial bit vibration. J. Petrol. Sci. Eng. 82, 140–150. https://doi.org/10.1016/j.petrol.2012.01.014.
Navarro-López, E.M., Cortés, D., 2007. Avoiding harmful oscillations in a drillstring through dynamical analysis. J. Sound Vib. 307 (1–2), 152–171. https://doi.org/10.1016/j.petrol.2012.01.014.
Oueslati, H., Jain, J.R., Reckmann, H., et al., 2013. New insights into drilling dynamics through high frequency vibration measurement and modeling. Proceedings-SPE Annual Technical Conference and Exhibition, pp. 1648–1662. https://doi.org/10.2118/166212-MS.
Popp, K., Panning, L., Sextro, W., 2003. Vibration damping by friction forces: theory and applications. J. Vib. Control 9 (3–4), 419–448. https://doi.org/10.1177/107754603030780.
Qin, K., Di, Q.F., Zhou, X., et al., 2022. Nonlinear dynamic characteristics of the drill-string for deep-water and ultra-deep water drilling. J. Petrol. Sci. Eng. 209, 109905. https://doi.org/10.1016/j.petrol.2021.109905.
Ritto, T.G., Soize, C., Sampaio, R., 2009. Non-linear dynamics of a drill-string with uncertain model of the bit–rock interaction. Int. J. Non Lin. Mech. 44 (8), 865–876. https://doi.org/10.1016/j.ijnonlinmec.2009.06.003.
Shi, X.L., Huang, W.J., Gao, D.L., 2021. Mechanical behavior of drillstring with drag reduction oscillators andits effects on sliding drilling limits. Pet. Sci. 18 (6), 1689–1697. https://doi.org/10.1016/j.petsci.2021.09.007.
Sivaram, N.M., 2023. Design and optimization of automotive cardan shafts for industrial applications with enhanced performance and durability. Babylonian Journal of Mechanical Engineering 1, 1–12. https://doi.org/10.58496/BJME/2023/001.
Tikhonov, V.S., Bukashkina, O.S., 2014. A new model of high-frequency torsional oscillations (HFTO) of drillstring in 3-D wells. SPE International Petroleum Technology Conference 2014, Kuala Lumpur, Malaysia. https://doi.org/10.2523/IPTC-17958-MS.
Tipples, R., Keshiyev, S., Sheikhrezaei, K., et al., 2021. Bit design methodology to mitigate high-frequency torsional oscillation. Proceedings-SPE Annual Technical Conference and Exhibition, pp. 1–19. https://doi.org/10.2118/206353-MS.
Wang, C.S., Ming, C.Z., Zhang, H., et al., 2024. Analysis of secondary makeup characteristics of drill collar joint and prediction of downhole equivalent impact torque of Well SDTK1. Petrol. Explor. Dev. 51 (3), 697–705. https://doi.org/10.1016/S1876-3804(24)60498-2.
Wang, N., Cheng, Z., Lu, Y., et al., 2015. A multibody dynamics model of contact between the drillstring and the wellbore and the rock penetration process. Adv. Mech. Eng. 7 (5), 1–12. https://doi.org/10.1177/1687814015582117.
Wang, S.R., 2006. Successive overrelaxation iteration method for solving sparse linear equations. J. Shanxi Normal Univ. (Philos. Soc. Sci. Ed.) (4), 407–410. https://doi.org/10.3969/j.issn.1673-5862.2006.04.007 (in Chinese).
Xi, Y., Wang, H.Y., Zha, C.Q., et al., 2023. Numerical simulation of rock-breaking and influence laws of dynamic load parameters during axial-torsional coupled impact drilling with a single PDC cutter. Pet. Sci. 20 (3), 1806–1827. https://doi.org/10.1016/j.petsci.2023.01.009.
Xu, G., 2002. The sufficient and necessary conditions of the convergence of SOR iterative method. Journal of Shandong Institute of Architecture and Engineering (4), 93–95 (in Chinese).
Yigit, A.S., Christoforou, A.P., 2000. Coupled torsional and bending vibrations of actively controlled drillstrings. J. Sound Vib. 234 (1), 67–83. https://doi.org/10.1006/jsvi.1999.2854.
Zhang, H., Di, Q.F., Li, N., et al., 2020. Measurement and simulation of nonlinear drillstring stick-slip and whirling vibrations. Int. J. Non Lin. Mech. 125, 1–14. https://doi.org/10.1016/j.ijnonlinmec.2020.103528.
Zhao, D., Hovda, S., Sangesland, S., 2016. The effect of stick slip vibration on the backward whirl of bottom hole assembly in drillstring. Int. Conf. Offshore Mech. Arctic Eng. 49996, V008T11A042. https://doi.org/10.1115/OMAE2016-54478.
Zhu, X.H., Liu, Q.Y., Tong, H., 2008. Research on dynamic model of 3D borehole whole drilling string system. Acta Pet. Sin. 29 (2), 288–291. https://doi.org/10.7623/syxb200802025.